



Article

Cite this article: Li C et al. (2021). Spatial and temporal variations of fractionation of stable isotopes in East-Antarctic snow. *Journal of Glaciology* 67(263), 523–532. <https://doi.org/10.1017/jog.2021.5>

Received: 3 June 2020

Revised: 18 January 2021

Accepted: 19 January 2021

First published online: 1 March 2021

Key words:

East Antarctica; fractionation; MWL slopes; stable isotopes

Author for correspondence:

Chuanjin Li, E-mail: lichuanjin@zb.ac.cn

Spatial and temporal variations of fractionation of stable isotopes in East-Antarctic snow

Chuanjin Li¹, Jiawen Ren¹, Guitao Shi^{2,3} , Hongxi Pang⁴, Yetang Wang⁵ , Shugui Hou⁴, Zhongqin Li¹, Zhiheng Du¹ , Minghu Ding^{1,6}, Xiangyu Ma¹, Jiao Yang¹, Aihong Xie¹ , Puyu Wang¹, Xiaoming Wang¹, Bo Sun³ and Cunde Xiao^{1,7}

¹State Key Laboratory of Cryospheric Science, Northwest Institute of Eco-Environment and Resources, Chinese Academy of Sciences, Lanzhou 730000, China; ²Key Laboratory of Geographic Information Science (Ministry of Education), School of Geographic Sciences and Institute of Eco-Chongming, East China Normal University, Shanghai 200241, China; ³Key Laboratory for Polar Science of State Oceanic Administration, Polar Research Institute of China, Shanghai 200062, China; ⁴School of Geography and Ocean Science, Nanjing University, Nanjing 210023, China; ⁵College of Geography and Environment, Shandong Normal University, Ji'nan 250358, China; ⁶Institute of Tibetan Plateau and Polar Regions Meteorology, Chinese Academy of Meteorological Sciences, Beijing 100081, China and ⁷State Key Laboratory of Earth Surface Processes and Resource Ecology, Beijing Normal University, Beijing 100875, China

Abstract

Stable isotope ratios ($\delta^{18}\text{O}$ and δD) in Antarctic snow and ice are basic proxy indices of climate in ice core studies. The relation between the ratios has important indicative significance for moisture sources. In general, the fractionation characteristics of the two isotopes vary with different meteorological and topographical conditions. This paper presents the spatial and temporal distribution of meteoric water line (MWL) slopes along a traverse from the Zhongshan Station (ZSS) to Dome A in East Antarctica. It is found that the slopes decrease with the increasing distance inland from the coast and the lowest slope occurred at Dome A, where the long-range transported moisture dominates and clear sky snowing have an influence. The slopes in different layers of the snowpack showed a decreasing trend with depth and this is attributed to the fractionation during the interstitial sublimation and re-condensation processes of the water vapor. Frost flower development on the interior plateau surface can greatly alter the depth evolution of the MWL slope. The coastal snow pits also go through the post-depositional smoothing effect, but their influences are not so significant as the inland regions.

Introduction

Stable isotope records of snow and ice cores in Antarctica were widely used to infer past local temperature variations and moisture origin (Dansgaard, 1964; Landais and others, 2008; Steen-Larsen and others, 2011; Xiao and others, 2013). The isotopic composition in snow, namely the ratio between its heavy and light water molecules, is expressed as δD or $\delta^{18}\text{O}$ relative to the Vienna Standard Mean Ocean Water (V-SMOW) reference (δD and $\delta^{18}\text{O}$, defined as $\delta\text{D} = (([\text{HD}^{16}\text{O}]/[\text{H}_2^{16}\text{O}])_{\text{sample}} / ([\text{HD}^{16}\text{O}]/[\text{H}_2^{16}\text{O}])_{\text{V-SMOW}} - 1) \times 1000$; $\delta^{18}\text{O} = (([\text{H}_2^{18}\text{O}]/[\text{H}_2^{16}\text{O}])_{\text{sample}} / ([\text{H}_2^{18}\text{O}]/[\text{H}_2^{16}\text{O}])_{\text{V-SMOW}} - 1) \times 1000$) (Craig, 1961; Dansgaard, 1964; Masson-Delmotte and others, 2008; Steen-Larsen and others, 2011). More recent ice core studies in Antarctica have been dedicated to obtaining the longest possible climate records in the Polar Regions (e.g., Jouzel and others, 2007), or characterizing at high-resolution structure of climate variability during glacial (Masson-Delmotte and others, 2003; EPICA Community Members, 2006; Stenni and others, 2010) or interglacial periods (Pol and others, 2011). Ongoing efforts are directed at documenting the regional variability of climate in various sectors of Antarctica and the related trajectories of air mass transportation and moisture origin. Triple oxygen isotopes (^{16}O , ^{17}O and ^{18}O) and double hydrogen isotopes (^1H and ^2H) and the second-order parameters (d-excess and ^{17}O -excess, calculations follow the equations $\text{d-excess} = \delta\text{D} - 8 \times \delta^{18}\text{O}$ and $^{17}\text{O}\text{-excess} = 10^6 (\ln(\delta^{17}\text{O}/1000 + 1) - 0.528 \times \ln(\delta^{18}\text{O}/1000 + 1))$), respectively) were widely involved to study the temporal and spatial variations of water isotopes (Dansgaard, 1964; Masson-Delmotte and others, 2003; Barkan and Luz, 2007; Hou and others, 2007, 2013; Landais and others, 2008; Xiao and others, 2013; Benetti and others, 2014; Pang and others, 2015, 2019). The isotopic content is strongly influenced by fractionation processes encountered by the air mass throughout its history, such as evaporation conditions, mixture of moisture sources and distillation of the air mass (Dansgaard, 1964; Masson-Delmotte and others, 2003, 2008; Steen-Larsen and others, 2015). The variations of the relationship between stable isotopes and the temperature arise from changes in ocean evaporation conditions such as sea surface temperatures (SST), relative humidity and ocean surface water isotopic composition (Bonne and others, 2019). When only the equilibrium isotopic fractionation occurs, a mean slope of 8.0 for $\delta\text{D}/\delta^{18}\text{O}$ of the precipitation will be presented. However, during non-equilibrium phase occurs, such as ocean surface evaporation processes, a kinetic fractionation effect is added to the equilibrium fractionation (Craig and Gordon, 1965), which causes a

© The Author(s), 2021. Published by Cambridge University Press. This is an Open Access article, distributed under the terms of the Creative Commons Attribution licence (<http://creativecommons.org/licenses/by/4.0/>), which permits unrestricted re-use, distribution, and reproduction in any medium, provided the original work is properly cited.

cambridge.org/jog

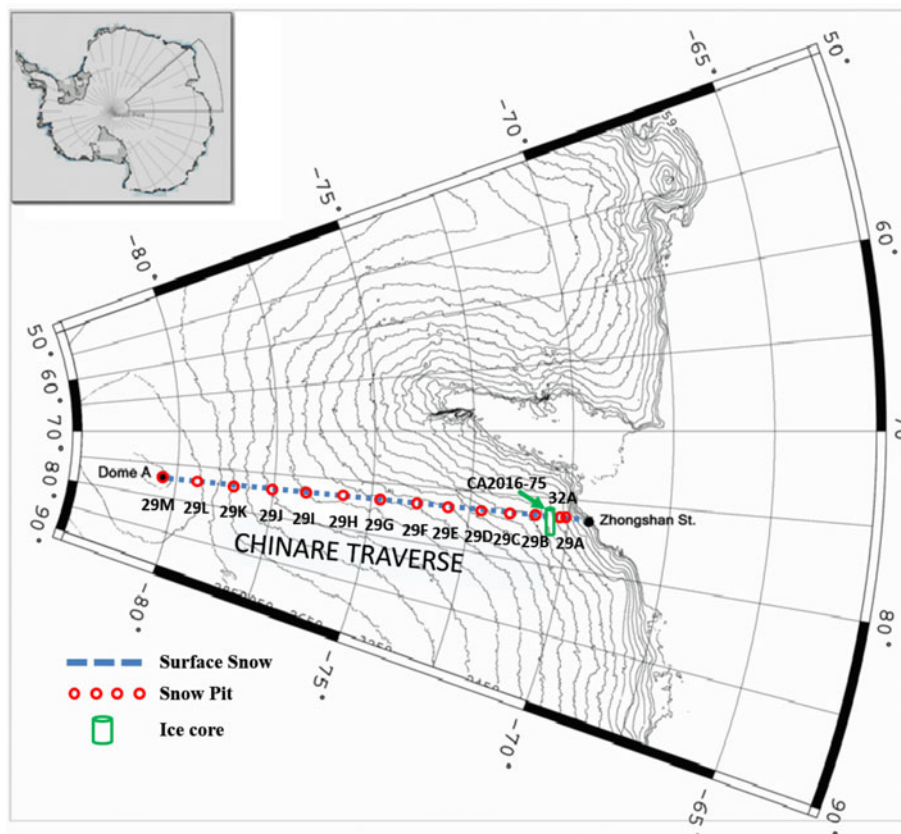


Fig. 1. Surface sampling sites along the CHINARE inland traverse between Zhongshan Station and Dome A. Red dots show the snow pit locations, the blue dotting line shows the surface sample sampling sites and the green column shows the location of the coastal ice core (CA2016-75).

larger kinetic fractionation for H_2^{18}O than for HDO due to their different molecular diffusivities. As a result, d-excess is strongly imprinted by the kinetic effect. Therefore, the calculation of the d-excess will provide independent isotopic information related to the initial air mass evaporation conditions at the ocean surface (mainly SST and relative humidity) (Merlivat and Jouzel, 1979; Bonne and others, 2019).

The mean slope between δD and $\delta^{18}\text{O}$ during the equilibrium fractionation (8.0) also known as the mean meteoric water line (MWL) was widely used to study the fractionation of the water isotopes in the worldwide precipitation (Dansgaard and others, 1964). However, a lower mean MWL slope (7.75) was detected on Antarctica ice sheet (Masson-Delmotte and others, 2008) and showed great spatial variations (Xiao and others, 2013; Li and others, 2016). The evaporation, transportation, condensation and the post-depositional processes on water vapor have influences on both the evolution of the water stable isotopes and MWL slopes (both for the equilibrium fractionation and kinetic fractionation) in Antarctic snowpack (Masson-Delmotte and others, 2008). The influencing factors at the deposition site mainly include the meteorological and topographical conditions (Xiao and others, 2013), precipitation type and intermittency (Cuffey and Steig, 1998; Helsen and others, 2006; Laepple and others, 2018), redistribution of snow (Ekaykin and others, 2002; Ekaykin and Lipenkov, 2009; Laepple and others, 2016; Münch and others, 2016), cyclones and cyclone paths (Qin and others, 1994), surface and interstitial sublimation and re-condensation processes (Ding and others, 2010, 2011; Steen-Larsen and others, 2013; Xiao and others, 2013; Madsen and others, 2019), etc. Calculations of the d-excess based on the routine MWL slope would result in great discrepancies in different sites. By now, few systematic studies on the spatial variations on MWL slopes were executed in Antarctica (Masson-Delmotte and others, 2008). In order to accurately interpret the stable water isotope records from deep ice cores, it is critical to evaluate the spatial

and temporal distribution of MWL slopes, which needs to be documented from modern measurements and processes studies (Xiao and others, 2013).

In addition, the influences of the fractionation on the initial deposition signals of the water isotopes and the alteration of climatic information were another research topic for inland Antarctic regions (Hoshina and others, 2014, 2016; Casado and others, 2016, Casado, 2018; Ritter and others, 2016). During the past decades, there existed some opposing views on what drives that deposition of water isotopes were due to climate variations or post-deposition noise. Some sites seemed to be greatly influenced by the signal (e.g., Dome F, Dome C and Vostok) while other sites were not (e.g. DML and South Pole) (Steen-Larsen and others, 2014; Münch and others, 2016). To make these controversial debates clear, more inland and coastal sites should be included and detailed studies on fractionation effects on temporal isotopic evolution process should be executed.

Here we present a modern process study on spatial and temporal variations of water stable isotopes ($\delta^{18}\text{O}$ and δD) in the snow along a traverse from coast to interior plateau in eastern Antarctica, and two topics are mainly involved: (1) spatial distribution of the MWL slopes at different sites with varied environmental and geographical conditions along the traverse and (2) the temporal variations of the MWL slopes in different depth of the snow pits and ice core and the possible causes for their spatial and temporal variations.

Samples and data

Samples and analysis

Dome A is located at the highest point of Eastern Antarctica ice sheet (4093 m) and 1248 km from the nearest coast (Fig. 1) (Hou and others, 2007; 2013; Xiao and others, 2008; 2013). According to in-situ measurement at the Dome A station (Hou

and others, 2007; Xiao and others, 2008; Ma and others, 2010), the mean annual temperature at Dome A is -58.5°C , the accumulation rate is 0.023 m a^{-1} w.e. and the mean wind velocity is 2.2 m s^{-1} . These values are the lowest among the stations in Antarctica. During the 29th Chinese National Antarctica Research Expedition (CHINARE) inland expedition from coastal Zhongshan Station (ZSS, $69^{\circ}37'31''\text{S}$, $76^{\circ}37'22''\text{E}$) to inland Dome A ($80^{\circ}25'01''\text{S}$, $77^{\circ}06'58''\text{E}$) in the austral summer in 2012/13, 13 snow pits and 115 surface samples were approximately evenly captured along the transect (Fig. 1 and Table 1) (Li and others, 2016). The depth of the snow pits varied from 2 to 3 m and the period covered changed from ~ 4 years at the coastal region to ~ 36 years at the interior regions. For the inland two snow pits (29-M and 29-L, Table 1), the mean sampling resolution was 3 cm, amounted to 0.3–0.4 year per sample depending on the density. The sampling depth for the surface samples along the traverse was 3–5 cm and the time covered varied from ~ 1 year in the interior regions to only the summer precipitation episodes at the coast. During the 32nd CHINARE inland expedition in 2015/16, another coastal snow pit (32-A) with larger depth (3 m) and higher sampling resolution (~ 4 cm per sample) was dug. During the same expedition, an ice core (CA2016-75) with the length 33.24 m were drilled (75 km from the coast) in a dry hole with a mechanical drill. The length, weight and diameter of each piece of ice core were measured just after its extraction.

All the samples were transported frozen to Lanzhou and all the analyzing procedures were executed at the State Key Laboratory of the Cryospheric Science (SKLCS) in Lanzhou China under 100–1000 class clean environment. Cations were analyzed on a Dionex ISC 3000 ion chromatograph (Dionex ISC 3000, Thermo Scientific, USA) using an Ion Pac CS12A column, 20 m mol L^{-1} MSA eluent and a cation electrolytically regenerated suppressor (CERS). The anions were analyzed on a Dionex ISC3000 ion chromatograph (Dionex ISC3000, Thermo Scientific, USA) using an Ion Pac AS11-HC column, 25 m mol L^{-1} KOH eluent, and an anion electrolytically regenerated suppressor (ASRS). The detection limit, defined as 3 times the standard deviation of the baseline noise, is $\sim 1\text{ ng g}^{-1}$ for all major ions. The stable isotope (D and ^{18}O) compositions of all samples were analyzed by a liquid-water isotope analyzer (DLT 100, Los Gatos, USA) based on off-axis integrated cavity output spectroscopy (OA-ICOS) at the SKLCS. The isotopic ratios are expressed in per mil (‰) units relative to Vienna Standard Mean Ocean Water (V-SMOW) (Xiao and others, 2013; Li and others, 2016). The accuracies of δD and $\delta^{18}\text{O}$ measurements are ± 0.6 and ± 0.2 ‰, respectively.

The linear second-order parameters on water isotopes of d-excess and the logarithmic d-excess (d-ln) are both adopted in this study to show their spatial and temporal variations and the related influencing factors and the calculation of d-ln is based on the equation: $\text{d-ln} = \ln(1 + \delta\text{D}) + 0.0285 (\ln(1 + \delta^{18}\text{O}))^2 - 8.47 \ln(1 + \delta^{18}\text{O})$ (Uemura and others, 2012; Markle and others, 2017).

Ancillary data

The coastal ice core (CA2016-75) was dated by the annual layer counting from the seasonal variation profiles of marine ions (Na^+ , SO_4^{2-}) and black carbon (BC). The separated dating results on Na^+ and BC are well consistent with the uncertainty of ± 2 years for 102 years (1915–2016 A.D.). The calculated annual mean accumulation rates on the ice core is $\sim 0.180\text{ m a}^{-1}$ w.e., met well with the previous results (Ding and others, 2011). The two inland snow pits (29-M and 29-L) were dated according to the volcanic deposit signals (Li and others, 2014) and the accumulation rate data. Because of the relative calm wind condition, the

influence of the drifting snow was negligible at Dome A. The calculated accumulation rates for the whole duration (37 years for 29-M and 36 years for 29-L) are consistent with the measurements by the automatic weather station (AWS) (Ma and others, 2010).

Results and Discussions

Spatial distribution of slopes along the transect

δD and $\delta^{18}\text{O}$ both show decreasing trends while d-excess increases with the distance from the coast along the ZSS to Dome A traverse (Xiao and others, 2013; Pang and others, 2015, 2019; Li and others, 2016). The mean slope of δD with the surface temperature was 6.4 ± 0.2 ‰ per $^{\circ}\text{C}$, like the average for East Antarctica (Masson-Delmotte and others, 2008; Xiao and others, 2013). The mean MWL slope in surface snow samples in this study (7.78 ± 0.04 , $R^2 = 0.99$) is little larger compared with the values measured before (7.5 ± 0.1 , $R^2 = 0.99$) along the same traverse (Xiao and others, 2013). We speculate the different sampling depth is responsible for the discrepancy. Our sampling depth (3–5 cm) is less compared with Xiao's study (5 cm) (Xiao and others, 2013).

According to the spatial variations of the accumulation rates and the impurities in snow (Ma and others, 2010; Ding and others, 2011; Xiao and others, 2013; Li and others, 2014, 2016; Shi and others, 2019; Ma and others, 2020), the ZSS-Dome A traverse can be divided the into three different sections, the coastal section (0–400 km), the intermediate section (400–900 km) and the interior section (900–1248 km). The mean slopes between δD and $\delta^{18}\text{O}$ in the coastal, intermediate and interior sections are 8.18 ± 0.15 ($R^2 = 0.99$, $n = 30$), 8.03 ± 0.09 ($R^2 = 0.99$, $n = 50$) and 7.79 ± 0.10 ($R^2 = 0.99$, $n = 35$), respectively. The general decreasing trend of the MWL slopes in three sections may be caused by the increasing distance from the source regions and intensified fractionation effects (Masson-Delmotte and others, 2008; Xiao and others, 2013; Pang and others, 2015, 2019).

To get a detailed spatial distribution pattern of the slopes along the traverse, the MWL slopes in the 13 snow pits were calculated (Fig. 2). In general, the slopes have a decreasing trend with the increasing distance inland. The snow pits located near the coast always show relatively higher slopes (Table 1) and the highest slope occurs in snow pit 29-C (8.61 ± 0.26 , $R^2 = 0.98$, $n = 20$) and this value was significantly larger than the global mean MWL (8.0) (Dansgaard and others, 1964) and also larger than the mean slope of the Antarctic snow (7.75 ± 0.02 , $R^2 = 0.998$) (Masson-Delmotte and others, 2008) (Fig. 2). Coastal regions of Antarctic ice sheet usually receive moisture from adjacent offshore water while the interior regions get sources from the distant open sea (Reijmer and others, 2002; Masson-Delmotte and others, 2008; Sodemann and Stohl, 2009). The higher MWL slopes at the coastal section may indicate less fractionation during the evaporation and the transportation processes (Hou and others, 2013; Xiao and others, 2013). In addition, the high accumulation at coastal section can cause a quick bury of the deposited snow, which is of benefit to stop (or reduce) the surface sublimation and condensation processes (Ding and others, 2010). The slopes in the intermediate section (400–900 km) generally show a 'V' spatial pattern and the slopes decrease at the initial part potentially implies a decrease of water vapor sources from the adjacent coastal ocean. However, after ~ 700 km, the slope shows an increasing trend till the ~ 900 km inland. We speculate that the intensified wind speed, special surface topography and the post-depositional effects may have influences to some extent (Xiao and others, 2013; Münch and others, 2016). The most interior snow pit at Dome A (29-M) has the lowest slope (7.24 ± 0.11 ,

Table 1. Statistics of the slopes of δD and $\delta^{18}O$ in snow samples along the ZSS-Dome A traverse^a

Sample information	Serial number	Location	Distance (km)	Elevation (m)	Depth (cm)	$\delta^{18}O$ (‰)	δD (‰)	Slope	Sample amount
Snow pits along the transect	29-M	80°22'00"S, 77°21'11"E	1248	4093	300	-58.46 ± 2.22	-450.93 ± 16.25	$\delta D = (7.24 \pm 0.11) \times \delta^{18}O - 27.61$ ($R^2 = 0.98$)	100
	29-L	79°05'57.1"S, 76°59'42.9"E	1100	3757	250	-55.02 ± 2.69	-425.97 ± 21.26	$\delta D = (7.84 \pm 0.10) \times \delta^{18}O + 5.88$ ($R^2 = 0.98$)	100
	29-K	77°59'51.1"S 77°06'42.2"E	976	3169	200	-47.25 ± 3.02	-368.40 ± 24.90	$\delta D = (8.20 \pm 0.11) \times \delta^{18}O + 19.28$ ($R^2 = 0.99$)	80
	29-J	77°12'2.7"S 76°58'3.7"E	886	2967	200	-48.52 ± 3.28	-380.33 ± 26.54	$\delta D = (8.05 \pm 0.10) \times \delta^{18}O + 10.23$ ($R^2 = 0.99$)	80
	29-I	76°20'45.2"S 77°02'14.4"E	792	2830	200	-45.01 ± 2.48	-356.09 ± 20.09	$\delta D = (7.95 \pm 0.36) \times \delta^{18}O + 1.68$ ($R^2 = 0.96$)	20
	29-H	75°27'0.7"S 76°53'42.6"E	690	2799	100	-46.15 ± 2.04	-363.22 ± 15.82	$\delta D = (7.65 \pm 0.47) \times \delta^{18}O - 10.22$ ($R^2 = 0.97$)	10
	29-G	73°54'52.7"S 76°59'15.6"E	520	2631	300	-40.60 ± 1.74	-321.91 ± 14.31	$\delta D = (8.11 \pm 0.18) \times \delta^{18}O + 7.24$ ($R^2 = 0.97$)	60
	29-F	73°26'7.1"S 76°59'20.7"E	466	2551	200	-42.25 ± 2.91	-333.98 ± 24.08	$\delta D = (8.21 \pm 0.22) \times \delta^{18}O + 12.99$ ($R^2 = 0.99$)	20
	29-E	72°51'27.2"S 77°22'31.9"E	400	2514	200	-38.09 ± 2.70	-301.16 ± 21.23	$\delta D = (7.82 \pm 0.20) \times \delta^{18}O - 3.18$ ($R^2 = 0.99$)	20
	29-D	71°58'42.8"S 77°56'45.3"E	300	2351	200	-37.23 ± 3.52	-297.10 ± 29.37	$\delta D = (8.32 \pm 0.18) \times \delta^{18}O + 12.59$ ($R^2 = 0.99$)	20
	29-C	71°11'12.7"S 77°21'52.2"E	210	2074	150	-33.81 ± 2.68	-268.41 ± 23.23	$\delta D = (8.61 \pm 0.26) \times \delta^{18}O + 22.55$ ($R^2 = 0.98$)	20
	29-B	70°30'11.9"S 76°49'36.5"E	130	1697	200	-28.87 ± 3.40	-226.04 ± 28.22	$\delta D = (8.27 \pm 0.20) \times \delta^{18}O + 12.60$ ($R^2 = 0.99$)	20
	29-A	69°42'39.5"S 76°28'43"E	40	832	200	-24.70 ± 1.93	-194.79 ± 16.35	$\delta D = (8.40 \pm 0.45) \times \delta^{18}O + 12.65$ ($R^2 = 0.98$)	8
	32-A	71°47'18.3"S 76°29'30"E	49	932	300	-25.42 ± 2.62	-197.91 ± 21.77	$\delta D = (8.27 \pm 0.09) \times \delta^{18}O + 12.35$ ($R^2 = 0.99$)	78
	Surface snow samples	Total	-	30-1248	622-4093	5	-40.95 ± 8.13	-321.69 ± 63.38	$\delta D = (7.78 \pm 0.04) \times \delta^{18}O - 3.10$ ($R^2 = 0.99$)
Interior		-	900-1248	3264-4093		-50.23 ± 4.51	-392.08 ± 34.87	$\delta D = (7.71 \pm 0.10) \times \delta^{18}O - 4.94$ ($R^2 = 0.99$)	35
middle		-	400-900	2516-3264		-39.66 ± 4.49	-313.19 ± 37.07	$\delta D = (8.23 \pm 0.09) \times \delta^{18}O + 13.16$ ($R^2 = 0.99$)	50
Coastal		-	30-400	622-2516		-32.26 ± 4.15	-253.75 ± 34.12	$\delta D = (8.18 \pm 0.15) \times \delta^{18}O + 10.11$ ($R^2 = 0.99$)	30
29-M	Upper	80°22'00"S, 77°21'11"E	1248	4093	0-100	-58.71 ± 2.84	-451.65 ± 21.49	$\delta D = (6.99 \pm 0.30) \times \delta^{18}O - 44.11$ ($R^2 = 0.95$)	33
	Middle				100-200	-58.62 ± 2.34	-451.24 ± 16.76	$\delta D = (7.14 \pm 0.14) \times \delta^{18}O - 32.75$ ($R^2 = 0.99$)	34
	Lower				200-300	-58.04 ± 1.11	-449.87 ± 7.96	$\delta D = (7.51 \pm 0.11) \times \delta^{18}O - 10.74$ ($R^2 = 0.99$)	33
29-L	Upper	79°05'57.1"S, 76°59'42.9"E	1100	3757	0-83	-55.48 ± 2.74	-430.22 ± 22.10	$\delta D = (8.01 \pm 0.18) \times \delta^{18}O + 14.32$ ($R^2 = 0.98$)	33
	Middle				84-167	-54.63 ± 2.83	-421.65 ± 22.47	$\delta D = (7.91 \pm 0.15) \times \delta^{18}O + 10.35$ ($R^2 = 0.99$)	34
	Lower				167-250	-55.05 ± 2.49	-426.82 ± 18.72	$\delta D = (7.44 \pm 0.18) \times \delta^{18}O - 17.05$ ($R^2 = 0.98$)	33
CA2016-75	Total	70°04'30"S, 77°07'03"E	75	1220	0-3324	-27.33 ± 1.85	-216.37 ± 14.14	$\delta D = (8.54 \pm 0.11) \times \delta^{18}O + 20.23$ ($R^2 = 0.98$)	799
	Upper				0-1000	-26.29 ± 2.04	-211.41 ± 15.81	$\delta D = (8.56 \pm 0.08) \times \delta^{18}O + 21.74$ ($R^2 = 0.99$)	236
	Lower				1000-3324	-27.77 ± 1.56	-218.45 ± 12.84	$\delta D = (8.37 \pm 0.09) \times \delta^{18}O + 15.81$ ($R^2 = 0.96$)	563

^aFor the detailed data and information, please refer to Fig. S1 and Table S1 to S16 in the supplementary materials.

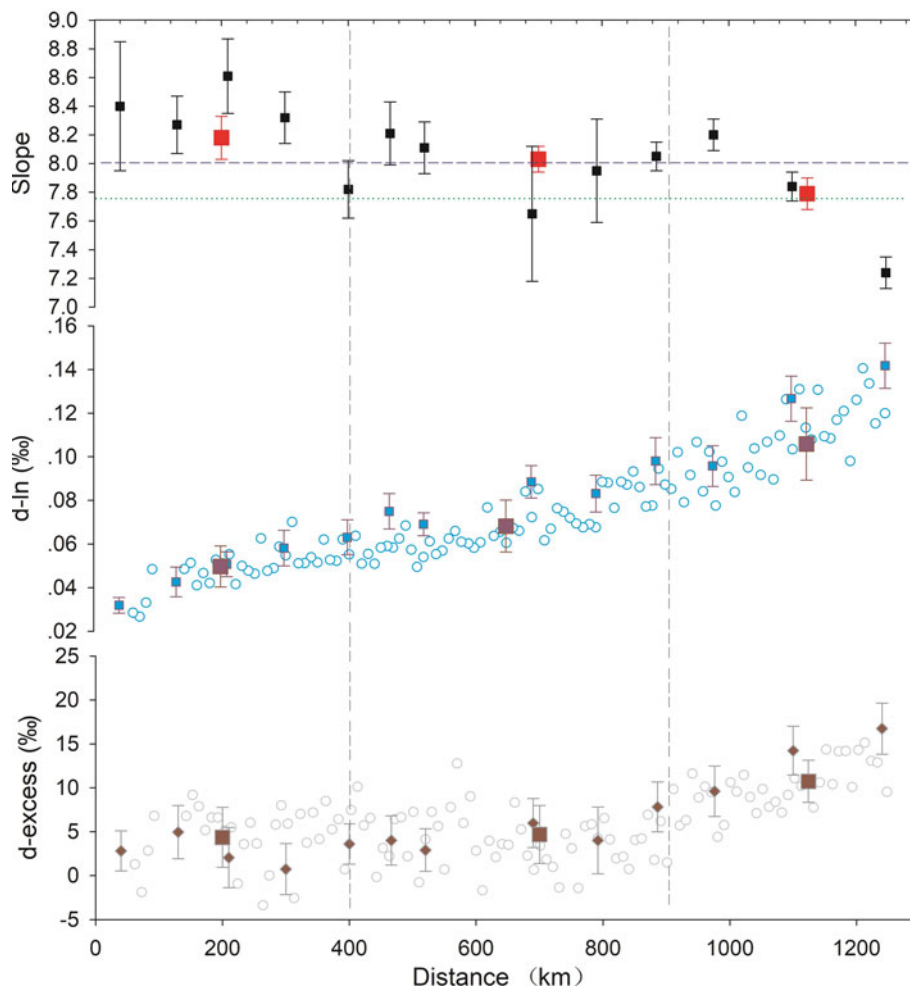


Fig. 2. Spatial distribution of the MWL (meteoric water line) between δD and $\delta^{18}O$ in 13 snow pits (29-M to 29-A, black square) and surface snow (red square) along the traverse from Zhongshan Station to Dome A together with the d-excess (bottom) and d-ln (middle). Different sections of the traverse are divided by the vertical dashed lines and the mean values of the parameters in different sections are shown in squares. The horizontal dotted lines show the global mean meteoritic water line (8.0, Dansgaard, 1964) and the mean slope in Antarctic snow (7.75, Masson-Delmotte and others, 2008).

$R^2 = 0.98$, $n = 100$), much lower than the global mean MWL and the Antarctic snow samples. Another interior snow pit 29-L also shows a low slope value (7.84 ± 0.10 , $R^2 = 0.98$, $n = 100$). The distance between the two sites is 148 km and they share similar environmental conditions (Ren and others, 1995, 2010).

In the previous studies, most interior snow samples usually show the lowest water isotope ratios (Masson-Delmotte and others, 2008; Xiao and others, 2013; Li and others, 2016). The water isotope ratios at the snow pit 29-M vary between -394.80 and -485.96‰ with the mean $-450.93 \pm 16.25\text{‰}$ for δD and between -63.25 and -50.67‰ with the mean $-58.46 \pm 2.22\text{‰}$ for $\delta^{18}O$. These values are the lowest in Antarctica up to date. Two potential reasons can be put forward to be mainly accountable for the lowest slope at the Dome A region. The first is the moisture source. The moisture arriving in the interior region is mainly from the low to mid-latitudes open oceans and has experienced long-distance transportation in the upper troposphere or lower stratosphere, and thus more intensive fractionation effects may occur during the long pathway (Xiao and others, 2013). The second is that at Dome A, low temperature together with the special precipitation form and accumulation have an intensifying effect on the surface evaporation and re-condensation of the water vapor at this highest location of Eastern Antarctica (Fujita and others, 2006; Ding and others, 2015). Clear sky precipitation (diamond dust) is particular in interior regions on the Antarctic ice sheet and can occupy a large fraction of the total accumulation (Hou and others, 2007). During the days with weak wind and higher temperature at the snow surface compared to the air, the vapor pressure of the air mass close to the snow surface can reach or even exceed saturation, resulting in frost flower growth

at the snow surface (Hou and others, 2007; Xiao and others, 2013). According to Hou and others (2007), the frost flower can comprise $\sim 7\%$ of the whole accumulation at Dome A. The diamond dust and frost flowers both present a large specific surface area ($300\text{--}590\text{ cm}^2\text{ g}^{-1}$) and hence are favorable to intensify the surface sublimation and re-condensation processes of water vapor. During the sublimation of ice grains and re-condensation of water vapor onto ice grains under extremely low temperatures, the isotopic fractionations will occur in the porous snow layers (Town and others, 2008; Wang and others, 2012; Hoshina and others, 2016; Casado and others, 2016, Casado, 2018; Madsen and others, 2019).

Comparison between the slopes and the mean d-excess values in the 13 snow pits shows that they have a generally opposite spatial variability ($R = -0.71$, $P < 0.01$, $N = 13$), the slopes decrease with the distance inland while the d-excess increase simultaneously (Fig. 2). They also show some different variation patterns at the coastal and the intermediate sections. The d-excess value in Antarctic snow is mainly controlled by the relative humidity, sea surface temperature and wind velocities at the moisture source regions (Hou and others, 2013; Bonne and others, 2019) and also influenced by the condensation conditions at the deposition site (Markle and others, 2017). The slope between δD and $\delta^{18}O$ is mainly controlled by the climatic and meteorological conditions of snowfall (air temperature, relative humidity, wind velocity, etc.) (Masson-Delmotte and others, 2008). Therefore, the difference between the slope and the d-excess may indicate that the local climatic and meteorological conditions had significant influences on the fractionation processes of the water isotopes. One point should be pointed out that the relation between the slopes

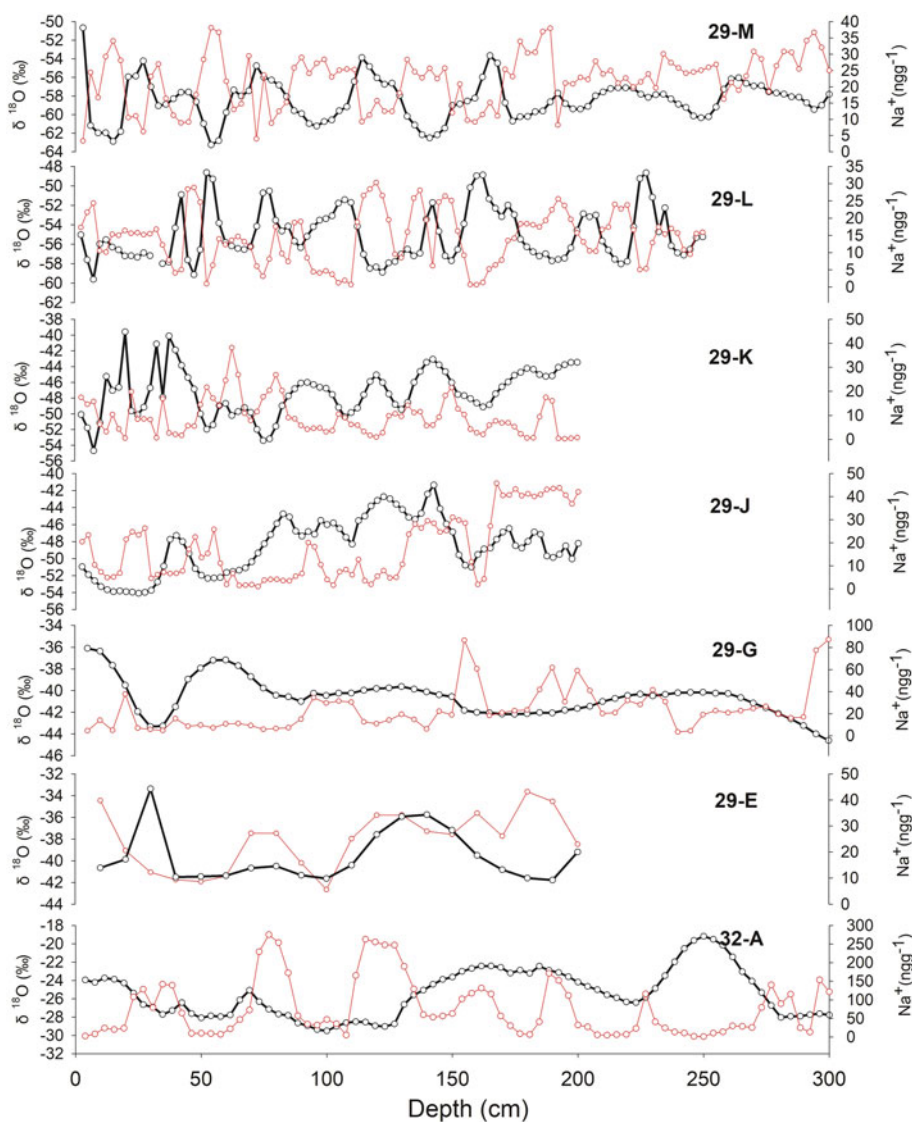


Fig. 3. Temporal variations of the $\delta^{18}\text{O}$ (black) and Na^+ (red) in different snow pits along the traverse between ZZS and Dome A.

and the source region conditions is mainly based on distillation modeling and future observations are in great demand to testify that (Masson-Delmotte and others, 2008).

The lognormal statistical on deuterium excess ($d\text{-ln}$) can effectively reduce the influences from the non-source factors and is regarded as an optimal index to study the climatic variations at the moisture source regions (Uemura and others, 2012; Markle and others, 2017). We made some comparisons among the slopes, $d\text{-excess}$ and the $d\text{-ln}$ values along the traverse (Fig. 2). The $d\text{-ln}$ clearly indicates a consistently increasing trend inland, implying a constant shift of different source regions and this is consistent with previous results (Masson-Delmotte and others, 2008; Xiao and others, 2013). The difference between the $d\text{-ln}$ and the slopes may be mainly caused by the influences from the local environment, especially on the intermediate section.

Temporal variations of water isotopes

The mean water isotopes (δD and $\delta^{18}\text{O}$) values in the 13 snow pits are systematically lower than the surface snow in the same areas, implying depleted isotope signals exist in the snow pits (Xiao and others, 2013; Li and others, 2016). We further investigate the temporal variations of the fractionation between δD and $\delta^{18}\text{O}$ in the snow pits and ice core. The temporal variations of the slopes in the two inland snow pits (29-M and 29-L) are firstly

investigated. The two pits are vertically divided into three parts (1 m resolution for 29-M and 0.83 m for 29-L). It shows a distinct increase ($K=0.26$, $P=0.15$) of the slope with depth in the 29-M (6.99 ± 0.30 , 7.14 ± 0.14 and 7.51 ± 0.11 for the top, middle and bottom sections, respectively), but 29-L shows an opposite variation pattern ($K=-0.29$, $P=0.23$) (8.01 ± 0.18 , 7.91 ± 0.15 and 7.44 ± 0.18 for the top, middle and bottom sections, respectively). This difference between the two snow pits should reflect the different fractionation processes at the two sites. During expeditions inland by the CHINARE, surface frost flower has been only seen at the 1150–1248 km on the traverse and no frost flower layer had been detected at 29-L. The fractionations of the water isotopes will sustain in the snow layer during the snow metamorphism and cause an increase of the isotopic composition in the upper layer. Isotope exchange and diffusion within the porous matrix of the snowpack affect snow isotopic composition (Langway, 1970; Johnsen, 1977; Ebner and others, 2017; Casado and others, 2018) and this procedure will be sustained until the firm transformation into ice. The different fractionation procedures between HDO and H_2^{18}O in the snowpack may be the causes for the increase of the slopes at the upper layers at 29-L (Masson-Delmotte and others, 2003). The inverse variations of the slopes at 29-M should be caused by the intensified fractionation effects on the frost flower with much lower slopes. The mixing effects within the surface snow will decrease the mean slope in

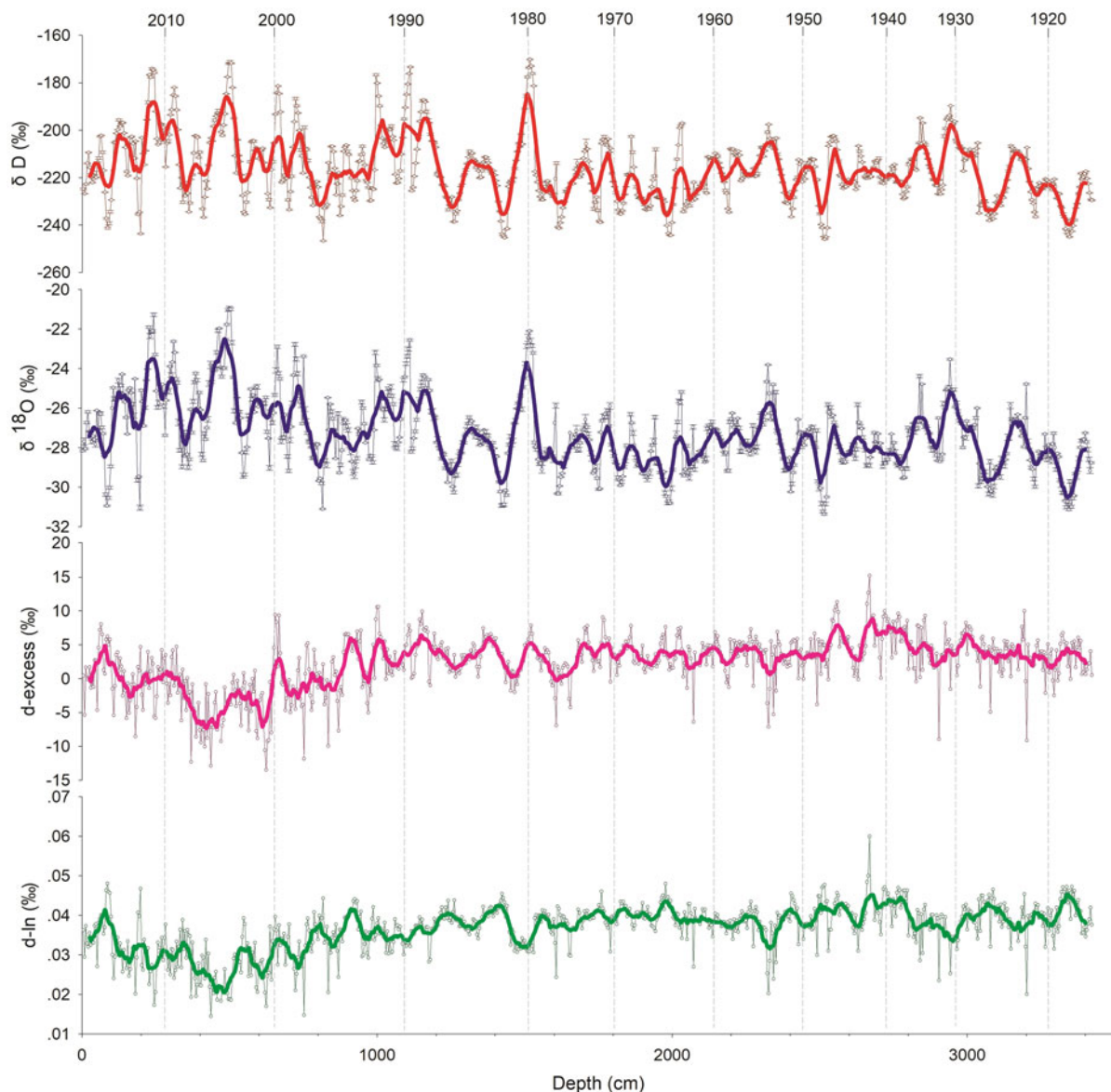


Fig. 4. Temporal variations of the δD (red), $\delta^{18}O$ (blue), d-excess (pink), d-ln (green) in the CA2016-75 ice core. The vertical dotted lines show the dating results of the ice core and the thick solid lines show the 10-point smoothing results (red for δD , blue for $\delta^{18}O$, pink for d-excess and green for d-ln, respectively).

the upper snow layers and the mixing effect decrease with depth can cause the slope increase. Because no surface frost flower is developed, no specific fractionation mechanism exists at the surface of 29-L, so the slope vertical variation shows an opposite pattern to 29-M, i.e. the slope decreases with depth at 29-L.

The vertical temperature gradients in different layers of the snow pits may be another important factor for the fractionation. The temperature gradient can cause the convection of the water vapor in the firn layers. Especially during the autumn and winter seasons, when the surface is significantly cooled down while the deeper layer still kept a relatively higher temperature, the water vapor sublimates at the lower depth can move upward and re-condenses at the shallower layers accompanied by the kinetic fractionation (Masson-Delmotte and others, 2008). The formation of depth hoar in the snow layers also has a great influence on the fractionation of water isotopes, especially at the sites in the inland with low accumulations (Satake and Kawada, 1997; Neumann and Waddington, 2004; Neumann and others, 2005). The widespread depth hoar in East Antarctic snow layers during the winter is a good proof for the interstitial sublimation and re-condensation processes (Qin and others, 1992, 1993; Ekaykin

and others, 2009). However, no depth hoar layers were observed in our snow pits since all the snow pits were dug in the summer season.

Previous studies on the variations of water isotopes with depth in the inland Antarctic snow pits (e.g. Vostok, Dome F, Dome C) showed a mean 20 cm cycle, and these intervals were ascribed to accumulation adjusting, wind erosion and post-depositional redistribution, which can significantly alter the initial seasonal depositional signals and climatic information (Hoshina and others, 2014, 2016; Casado and others, 2016; Laepple and others, 2016; Casado, 2018). We check the deposition signals of $\delta^{18}O$ in the snow pits along the traverse and find a similar variation pattern (Fig. 3). The two interior snow pits display the cycle periodicity varied between 16 and 51 cm with the mean value 32.38 ± 11.36 cm at 29-M and between 10 and 34 cm with the mean value of 23.89 ± 8.95 cm at 29-L. Moreover, both the snow pits show enlarged cycle periodicity with the depth accompanied by the decreasing variation amplitudes, implying that the smoothing effects of the isotopes is intensified with depth. The smoothing effects on the water stable isotopes with the depth can also be seen at the coastal and intermediate sections (Fig. 3). 29-G

shows an extreme smoothing trend in the bottom part, suggesting that besides the interstitial sublimation and re-condensation effects, the intensified wind erosion and mixing effects on the snow have great influences on the variations of the isotopes at this site. Sodium (Na^+) is usually regarded as a good indicator of the seasonal variations of the marine incursion, but its seasonal signals seem to be smoothed at the inland snow layers with similar depth intervals to the water isotopes (Fig. 3). Opposite variation patterns between the Na^+ and the water isotopes always exist generally in our inland snow pits and this phenomenon seems widespread among the eastern Antarctica (Hoshina and others, 2016). However, at the coastal snow pits, such as 32-A, Na^+ has clear seasonal variations but the water isotopes do not.

Because of the smoothing influences on the water isotopes in the inland snow pits, we select the ice core (CA2016-75) at the coastal region to study the annual variations of the water isotopes and the potential influencing factors (Fig. 4). The CA2016-75 ice core drilling site has a relatively high accumulation rate ($\sim 0.18 \text{ m a}^{-1}$ w.e.) and thickness of annual layers vary between 30 and 40 cm, so the annual mean depth usually has seven–ten samples and is sufficient to study the seasonal variations. Based on the dating results, the annual mean water isotopes and the second-order proxies (d-excess and d-ln) are calculated (Fig. 4). The seasonal variations of the $\delta^{18}\text{O}$ and δD can be detected for the top 10 m depth (since $\sim 1990\text{s}$). The smoothing effect is significantly below 10 m depth, eliminating the annual and seasonal signals. From this phenomenon, we can find the post-depositional sublimation and re-condensation of the water vapor is also significant in the coastal region, even for the sites with the high accumulation rates.

The MWL slope for the whole ice core (8.54 ± 0.11) is similar with the coastal 29-A and 32-A snow pits and a decrease of the slopes with depth is also detected (8.56 ± 0.08 for the upper 10 m and 8.37 ± 0.09 for the lower 23.24 m, Table 1). The temporal variability of water isotopes at CA2016-75 ice core is different from the Law Dome ice core (DE08-2) which shows significant seasonal cycles till 150 m depth (Masson-Delmotte and others, 2003). Higher accumulation for DE08-2 ice core site (between 1.00 and 1.50 m a^{-1} w.e.) and lower wind speed may be the dominant factors for the good preservation of the seasonal cycles of water isotopes in the ice core (Masson-Delmotte and others, 2003).

Variations of water isotope ratios (δD , $\delta^{18}\text{O}$, Fig. 4) show a general flat pattern between 1910s and mid-1980s, after that significant increases during 1980s–90s ($K = 2.89$, $P < 0.0001$, $N = 92$ for δD and $K = 0.36$, $P < 0.0001$, $N = 92$ for $\delta^{18}\text{O}$, respectively) and the ratios stay at a relatively higher level till the sampling time. The d-excess and d-ln show similar temporal variations for the whole duration (mid-1910s–2015A.D.) (Fig. 4). They both show relatively flat variations between 1910s and 1990s, and significant decreasing trends are followed till the mid-2000s and then a quick increasing trend till the sampling time. The reasons for the variations and variability of the isotopes and the second-order parameters (d-excess and d-ln) are beyond the scope of this paper and more detailed discussions will be included in the following studies.

Conclusions

Spatial and temporal distributions of fractionation slopes between δD and $\delta^{18}\text{O}$ in the surface snow, snow pits and ice core samples along the traverse from ZSS to Dome A were calculated. Three spatial sections were divided along the traverse, the low slope existed at the interior section and high values at the coastal region, the intermediate section showed large variations implying that complex mechanisms were involved in the fractionation processes

and more efforts are needed in the future. The lowest slope existed at Dome A and was much lower than the mean MWL, it was speculated that the long-range transportation of moisture to this interior plateau and the particular precipitation and accumulation styles at Dome A are the dominant influencing factors. Inland snow pits showed significant smoothing effects on the water isotopes as ever been found in other inland sites (Vostok, Dome C, Dome F, etc.) in eastern Antarctica and the original deposition signals of the water isotopes has been significantly altered. Moreover, not only the inland snow pits, the coastal snow pits in our study were also found for the post-depositional smoothing effects. The persistent sublimation, migration, and re-condensation of the water vapor in the snow (firn) layers caused by the deviations of the temperature in different depths and the wind sweeping effects may be the main influencing factors. The slopes of the isotopes in different depth changed significantly. Variations of the slopes with depth at Dome A snow pit (29-M) showed opposite distribution pattern to 29-L and the existence of the frost flower or not may be mainly accountable for the discrepancy. Coastal snow pits and ice cores showed different smoothing effects on the snow impurities which presented significant seasonal variations and multi-year oscillation. More efforts on other water isotopes tracers (e.g. $\delta^{17}\text{O}$ and tritium) in the near future are in demand to study the sources of the moisture along the traverse between ZSS and Dome A and their fractionation procedures under different environmental conditions and also for their relationships with the climatic variations.

Supplementary material. The supplementary material for this article can be found at <https://doi.org/10.1017/jog.2021.5>

Acknowledgement. We thank all the members who participated in the 2012/13 and 2016/17 CHINARE field campaigns for sample collection. Special thanks should also be given to analyzing personnel on the water isotopes in the State Key Laboratory of the Cryospheric Sciences. Dr Xiaoqing Cui, Ms. Xiaoxiang Wang, Yan Liu and Tingting Su and Yuman Zhu from the cold and arid region environmental and engineering research institute, Chinese Academy of Sciences who completed parts of the analysis. This work is financially supported by the Innovative Research Group, the National Natural Science Foundation of China (No. 41671063, 41830647, 41625012, and 41961144028), the State Key Laboratory of Cryospheric Sciences (supporting fund No. SKLCS-ZZ-2018-01) and the Youth Innovation Promotion Association, Chinese Academy of Sciences.

References

- Barkan E and Luz B** (2007) Diffusivity fractionations of $\text{H}_2^{16}\text{O}/\text{H}_2^{17}\text{O}$ and $\text{H}_2^{16}\text{O}/\text{H}_2^{18}\text{O}$ in air and their implications for isotope hydrology. *Rapid Communication Mass Spectrom* **21**, 2999–3005. doi: [10.1002/rcm.3180](https://doi.org/10.1002/rcm.3180)
- Benetti M and 6 others** (2014) Deuterium excess in marine water vapor: dependency on relative humidity and surface wind speed during evaporation. *Journal of Geophysical Research: Atmospheres* **119**(2), 584–593.
- Bonne JL and 9 others** (2019) Resolving the controls of water vapour isotopes in the Atlantic sector. *Nature Communications* **10**, 1632.
- Casado M** (2018) *Antarctic Stable Isotopes, Reference Module in Earth Systems and Environmental Sciences*. Amsterdam: Elsevier. doi: [10.1016/B978-0-12-409548-9.11655-0](https://doi.org/10.1016/B978-0-12-409548-9.11655-0).
- Casado M and 12 others** (2016) Continuous measurements of isotopic composition of water vapour on the East Antarctic Plateau. *Atmospheric Chemistry and Physics* **16**, 8521–8538.
- Craig H** (1961) Isotopic variation in meteoric water. *Science* **133**(3465), 1702–1703.
- Craig H and Gordon LI** (1965) Deuterium and oxygen 18 variations in the ocean and the marine atmosphere. In Tongiogi E (ed.), *Stable Isotopes in Oceanographic Studies and Paleotemperatures*. Pisa, Spoleto, Italy: V. Lishi e F., pp. 9–130.
- Cuffey KM and Steig EJ** (1998) Isotopic diffusion in polar firn: implications for interpretation of seasonal climate parameters in ice core records, with emphasis on central Greenland. *Journal of Glaciology* **44**, 273–284.
- Dansgaard W** (1964) Stable isotopes in precipitation. *Tellus* **16**, 436–468.

- Ding M and 5 others** (2010) Distribution of $\delta^{18}\text{O}$ in surface snow along a transect from Zhongshan Station to Dome A, East Antarctica. *Chinese Science Bulletin* **55**(24), 2709–2714.
- Ding M and 6 others** (2011) Spatial variability of surface mass balance along a traverse route from Zhongshan station to Dome A, Antarctica. *Journal of Glaciology* **57**(204), 658–666.
- Ding M and 8 others** (2015) Surface mass balance and its climate significance from the coast to Dome A, East Antarctica. *Science in China: Earth Science* **58**, 1787–1797. doi: [10.1007/s11430-015-5083-9](https://doi.org/10.1007/s11430-015-5083-9)
- Ebner PP, Steen-Larsen HC, Stenni B, Schneebeli M and Steinfeld A** (2017) Experimental observation of transient $\delta^{18}\text{O}$ interaction between snow and advective airflow under various temperature gradient conditions. *The Cryosphere* **11**, 1733–1743.
- Eckaykin AA and Lipenkov VY** (2009) Formation of the ice core isotopic composition. *Physics of ice core records, Low Temperature Science* **68** (Supplement), 299–314.
- Eckaykin AA, Lipenkov VY, Barkov NI, Petit JR and Masson-Delmotte V** (2002) Spatial and temporal variability in isotope composition of recent snow in the vicinity of Vostok Station, Antarctica: implications for ice-core record interpretation. *Annals of Glaciology* **35**(1), 181–186.
- EPICA Community Members** (2006) One-to-one coupling of glacial climate variability in Greenland and Antarctica. *Nature* **444**(7116), 195–198.
- Fujita K and Abe O** (2006) Stable isotopes in daily precipitation at Dome Fuji, East Antarctica. *Geophysical Research Letters* **33**, L18503. doi: [10.1029/2006GL026936](https://doi.org/10.1029/2006GL026936)
- Helsen MM and 6 others** (2006) Modeling the isotopic composition of Antarctic snow using backward trajectories: simulation of snow pit records. *Journal of Geophysical Research* **111**, D15109. doi: [10.1029/2005JD006524](https://doi.org/10.1029/2005JD006524)
- Hoshina Y and 8 others** (2014) Effect of accumulation rate on water stable isotopes of near-surface snow in inland Antarctica. *Journal of Geophysical Research - Atmosphere* **119**, 274–283.
- Hoshina Y, Fujita K, Iizuka Y and Motoyama H** (2016) Inconsistent relationships between major ions and water stable isotopes in Antarctic snow under different accumulation environments. *Polar Sciences* **10**, 1–10.
- Hou S, Li Y, Xiao C and Ren J** (2007) Recent accumulation rate at Dome A, Antarctica. *Chinese Science Bulletin* **52**, 428–431.
- Hou S, Wang Y and Pang H** (2013) Climatology of stable isotopes in Antarctic snow and ice: Current status and prospects. *Chinese Science Bulletin* **58**, 1095–1106.
- Johnsen S** (1977) Stable isotope homogenization of polar firn and ice, in Proc. of Symp. on Isotopes and Impurities in Snow and Ice, I.U.G.G. XVI, General Assembly, Grenoble, pp. 210–219, IAHS-AISH Publ. 118.
- Jouzel J and 31 others** (2007) Orbital and millennial Antarctic climate variability over the past 800000 years. *Science* **317**, 793–796.
- Laepfle T and 5 others** (2016) Layering of surface snow and firn at Kohnen Station, Antarctica: noise or seasonal signal? *Journal of Geophysical Research-Earth Surface* **121**, 1849–1860.
- Laepfle T and 5 others** (2018) On the similarity and apparent cycles of isotopic variations in East Antarctic snow pits. *The Cryosphere* **12**, 169–187.
- Landais A, Barkan E and Luz B** (2008) The record of $\delta^{18}\text{O}$ and $\delta^{17}\text{O}$ excess in ice from Vostok, Antarctica, during the last 150 000 years. *Geophysical Research Letters* **35**, L02709. doi: [10.1029/2007GL032096](https://doi.org/10.1029/2007GL032096)
- Langway CC** (1970) *Stratigraphic analysis of a deep ice core from Greenland*, Special Paper 125. Boulder, CO: The Geological Society of America.
- Li C and 8 others** (2014) Temporal variations in marine chemical concentrations in coastal areas of eastern Antarctica and associated climatic causes. *Quaternary International* **352**, 16–25.
- Li C and 5 others** (2016) Spatial and temporal variability of marine-origin matter along a transect from Zhongshan Station to Dome A, Eastern Antarctica. *Journal of Environmental Sciences* **46**, 190–202.
- Ma X and 11 others** (2020) Spatial and temporal variations of refractory black carbon along the transect from Zhongshan Station to Dome A, eastern Antarctica. *Atmospheric Environment* **242**, 117816.
- Ma Y, Bian L, Xiao C, Allison I and Zhou X** (2010) Near surface climate of the traverse route from Zhongshan Station to Dome A, East Antarctica. *Antarctic Science* **22**(04), 443–459.
- Madsen MV and 9 others** (2019) Evidence of isotopic fractionation during vapor exchange between the atmosphere and the snow surface in Greenland. *Journal of Geophysical Research-Atmospheres* **124**, 2932–2945. doi: [10.1029/2018JD029619](https://doi.org/10.1029/2018JD029619)
- Markle BR and 9 others** (2017) Global atmospheric teleconnections during Dansgaard-Oeschger events. *Nature Geoscience* **10**(1), 36–40. doi: [10.1038/ngeo2848](https://doi.org/10.1038/ngeo2848)
- Masson-Delmotte V and 6 others** (2003) Recent southern Indian ocean climate variability inferred from a Law Dome ice core: new insights for the interpretation of coastal Antarctic isotopic records. *Climate Dynamics* **21**, 153–166.
- Masson-Delmotte V and 35 others** (2008) A review of Antarctic surface snow isotopic composition: observations, atmospheric circulation, and isotopic modeling. *Journal of Climate* **21**, 3359–3387.
- Merlivat L and Jouzel J** (1979) Global climatic interpretation of the deuterium-oxygen 18 relationship for precipitation. *Journal of Geophysical Research* **84**, 5029–5033. doi: [10.1029/JC084iC08p05029](https://doi.org/10.1029/JC084iC08p05029)
- Münch T, Kipfstuhl S, Freitag J, Meyer H and Laepfle T** (2016) Regional climate signal vs. Local noise: a two-dimensional view of water isotopes in Antarctic firn at Kohnen Station, Dronning Maud Land. *Climate of the Past* **12**, 1565–1581.
- Neumann TA and Waddington ED** (2004) Effects of firn ventilation on isotopic exchange. *Journal of Glaciology* **50**, 183–194. doi: [10.3189/172756504781830150](https://doi.org/10.3189/172756504781830150)
- Neumann TA, Waddington ED, Steig EJ and Grootes PM** (2005) Non-climate influences on stable isotopes at Taylor Mouth, Antarctica. *Journal of Glaciology* **51**, 248–258.
- Pang H and 12 others** (2015) Spatial distribution of ^{17}O -excess in surface snow along a traverse from Zhongshan station to Dome A, East Antarctica. *Earth and Planetary Science Letters* **44**, 126–133.
- Pang H and 18 others** (2019) Influence of summer sublimation on δD , $\delta^{18}\text{O}$, and $\delta^{17}\text{O}$ in precipitation, East Antarctica, and implications for climate reconstruction from ice cores. *Journal of Geophysical Research: Atmospheres* **124**, 7339–7358.
- Pol K and 11 others** (2011) Links between MIS 11 millennial to sub-millennial climate variability and long-term trends as revealed by new high-resolution EPICA Dome C deuterium data – a comparison with the Holocene. *Climate of the Past* **7**(2), 437–450.
- Qin D, Petit JR, Jouzel J and Stievenard M** (1994) Distribution of stable isotopes in surface snow along the route of the 1990 International Trans-Antarctica Expedition. *Journal of Glaciology* **40**(134), 107–118.
- Qin D and Ren J** (1992) A study on snow profiles and surface characteristics along 6000km Trans-Antarctic route. *Science in China* **35**(3), 366–374.
- Qin D, Ren J, Wang W, Petit JR and Jouzel J** (1993) Distribution of δD in 25-cm surface snow along Trans-Antarctic Route (II) – the “1990 International Trans-Antarctic Expedition” glaciological research. *Science in China* **36**(3), 375–384.
- Reijmer CH, Van den Broeke MR and Scheele MP** (2002) Air parcel trajectories and snowfall related to five deep drilling locations in Antarctica based on the ERA-15 dataset. *Journal of Climate* **15**, 1957–1968.
- Ren J and 6 others** (2010) A 2680 year volcanic record from the DT-401 East Antarctic ice core. *Journal of Geophysical Research* **115**(D11), D11301. doi: [10.1029/2009JD012892](https://doi.org/10.1029/2009JD012892)
- Ren J and Qin D** (1995) Distribution of deuterium excess in surface snow of the Antarctic ice sheet. *Chinese Scientific Bulletin* **40**(19), 1629–1633.
- Ritter F and 9 others** (2016) Isotopic exchange on the diurnal scale between near-surface snow and lower atmospheric water vapor at Kohnen station, East Antarctica. *The Cryosphere* **10**, 1647–1663. doi: [10.5194/tc-10-1647-2016](https://doi.org/10.5194/tc-10-1647-2016)
- Satake H and Kawada K** (1997) The quantitative evaluation of sublimation and the estimation of original hydrogen and oxygen isotope ratios of a firn core at East Queen Maud Land, Antarctica. *Bulletin of Glacier Research* **15**, 93–97.
- Shi G and 9 others** (2019) Organic tracers from biomass burning in snow from the coast to the ice sheet summit of East Antarctica. *Atmospheric Environment* **201**, 231–241.
- Sodemann H and Stohl A** (2009) A symmetries in the moisture origin of Antarctic precipitation. *Geophysical Research Letters* **36**, L22803. doi: [10.1029/2009GL040242](https://doi.org/10.1029/2009GL040242)
- Steen-Larsen HC and 23 others** (2011) Understanding the climatic signal in the water stable isotope records from the NEEM shallow firn/ice cores in northwest Greenland. *Journal of Geophysical Research* **116**, D06108. doi: [10.1029/2010JD014311](https://doi.org/10.1029/2010JD014311)
- Steen-Larsen HC and 23 others** (2013) Continuous monitoring of summer surface water vapor isotopic composition above the Greenland Ice Sheet. *Atmospheric Chemistry and Physics* **13**, 4815–4828.

- Steen-Larsen HC and 18 others** (2014) What controls the isotopic composition of Greenland surface snow? *Climate of the Past* **10**, 377–392.
- Steen-Larsen HC and 9 others** (2015) Moisture sources and synoptic to seasonal variability of North Atlantic water vapor isotopic composition. *Journal of Geophysical Research: Atmosphere* **120**, 5757–5774.
- Stenni B and 14 others** (2010) The deuterium excess records of EPICA Dome C and Dronning Maud Land ice cores (East Antarctica). *Quaternary Science Reviews* **29**, 146–159.
- Town MS, Warren SG, Walden VP and Waddington ED** (2008) Effect of atmospheric water vapor on modification of stable isotopes in near-surface snow on ice sheets. *Journal of Geophysical Research* **113**, D24303. doi: [10.1029/2008JD009852](https://doi.org/10.1029/2008JD009852)
- Uemura R and 5 others** (2012) Ranges of moisture-source temperature estimated from Antarctic ice cores stable isotope records over glacial–interglacial cycles. *Climate of the Past* **8**, 1109–1125.
- Wang Y and 5 others** (2012) Snow accumulation and its moisture origin over Dome Argus, Antarctica. *Climate Dynamics* **40**, 731–742. doi: [10.1007/s00382-012-1398-9](https://doi.org/10.1007/s00382-012-1398-9).
- Xiao C and 5 others** (2008) Preliminary evidence indicating Dome A (Antarctica) satisfying pre conditions for drilling the oldest ice core. *Chinese Science Bulletin* **53**, 102–106.
- Xiao C and 10 others** (2013) Stable isotopes in surface snow along a traverse route from Zhongshan station to Dome A, East Antarctica. *Climate Dynamics* **41**, 2427–2438. doi: [10.1007/s00382-012-1580-0](https://doi.org/10.1007/s00382-012-1580-0)